Polymer 50 (2009) 3292–3301

Contents lists available at ScienceDirect

Polymer

journal homepage: www.elsevier.com/locate/polymer

Composite nanofibers of conducting polymers and hydrophobic insulating polymers: Preparation and sensing applications

Hua Bai [a], Lu Zhao [a], Canhui Lu [b], Chun Li [a], Gaoquan Shi [a,*]

[a] Key Laboratory of Bioorganic Phosphorus Chemistry and Chemical Biology, Department of Chemistry, Tsinghua University, Beijing 100084, PR China
[b] State Key Laboratory of Polymer Materials Engineering, Sichuan University, Chengdu 610064, PR China

ARTICLE INFO

Article history:
Received 17 October 2008
Received in revised form
3 April 2009
Accepted 29 April 2009
Available online 8 May 2009

Keywords:
Conducting polymer nanofiber
Electrospinning
Vapor deposition polymerization

ABSTRACT

Various conducting polymer/hydrophobic insulating polymer (CP/HIP) composite nanofibers have been prepared by electrospinning and vapor deposition polymerization (VDP) with benzoyl peroxide (BPO) as oxidant. BPO is soluble in *N*,*N*-dimethylformamide (DMF) and can form homogenous solutions with hydrophobic polymers such as poly(methyl methacrylate) (PMMA) and polystyrene (PS). High-quality nanofibers of PMMA or PS containing a certain amount of BPO were produced by electrospinning and used as the templates for VDP of pyrrole, 3,4-ethylenedioxythiophene (EDOT), and aniline. The non-woven mats of the resulting CP/HIP composite fibers can be used as the high-sensitive sensing elements of gas sensors. A gas senor based on polypyrrole (PPy)/PMMA composite fibers was fabricated for sensing ammonia or chloroform vapor, and exhibited greatly improved performances comparing with those of the device based on a PPy flat film.

1. Introduction

One-dimensional (1D) conducting polymeric (CP) materials, such as nanofibers, nanotubes, and nanowires have attracted a great deal of attention in these years [1–10]. This is mainly due to their unique morphologies, conductive and redox properties, and the applications in drug delivery [1,2], electric devices [3,4], actuators [5,6] and especially chemosensors [7–10]. Among these materials, 1D CP composites are of special importance because of the intriguing properties inherited from the synergistic effect of their components except for the intrinsic properties from each component [11]. For example, polypyrrole/single-walled carbon nanotube (PPy/SWCNT) bi-component nanocables exhibited a conductive behavior different from that predicted by parallel conduction-channel model [12].

1D CP composites can be prepared by various techniques such as template-assisted polymerization [12–20], lithography [21], interfacial polymerization [22], and electrospinning [23–30], leading to the formation of two kinds of structures: blends and coaxial cables. Usually, the coaxial cable structured composites are prepared through two-step processes. For example, PPy/PMMA coaxial nanocables were synthesized by sequential polymerizations of methyl methacrylate and pyrrole inside the channels of mesoporous silica [31]. The nanocables of CPs also can be prepared by chemical deposition of CP on the surfaces of electrospun fibers [32,33]. However, the synthesis of 1D blend is more difficult, mainly due to the fact that most CPs are insoluble in common solvents. Thus, the solvent-assisted methods usually used for preparing polymer composites are inapplicable to the preparation of CP composites. Although a few strategies have been developed for producing CP blending films or powders [34,35], they are not suitable for the preparation of corresponding 1D nanomaterials.

Recently, it was reported that vapor deposition polymerization (VDP) of pyrrole can be carried out on the electrospun composite fibers of polyethylene glycol (PEG) containing inorganic oxidant such as ferric chloride, resulting in the formation of PPy/PEG fibers [36,37]. Although the distribution of PPy in the PEG matrix was not described, it is reasonable to conclude that VDP occurs within the PEG fiber matrixes, leading to the formation of the blends of PPy and PEG. However, this strategy is limited to prepare CP/hydrophilic polymer composite fibers on account of the difficulty of incorporating water-soluble inorganic oxidants (e.g. ferric chloride, ammonia persulphate) into hydrophobic matrixes. Recently, a few papers reported the preparation of 1D CP composite nanofibers by using the electrospun composite fibers of organic ferric salt and polystyrene (PS) as the templates [38,39]. Unfortunately, in these cases, the quality of the obtained CP composite fibers was poor (short and wide), and the electrospin systems needed careful optimization in order to ensure the solubility of both components, as well as the spinnability of the solutions. Therefore, hitherto, there is not a convenient universal strategy for the fabrication of high-quality 1D blends of CPs and hydrophobic insulating polymers.

* Corresponding author. Tel.: +86 1062773743; fax: +86 1062771149.
E-mail address: gshi@tsinghua.edu.cn (G. Shi).

0032-3861/$ – see front matter © 2009 Elsevier Ltd. All rights reserved.
doi:10.1016/j.polymer.2009.04.066

In this paper, we report the preparation of CP/hydrophobic insulating polymer (HIP) composite fibers by using benzoyl peroxide (BPO) as a liposoluble oxidant for VDP. BPO/HIP composite fibers were prepared by electrospinning, and VDP of pyrrole was carried out on the matrixes of the electrospun fibers. BPO has been used as oxidant for chemical polymerization of pyrrole [40] and has good solubility in many organic solvents. Thus, the mixture solutions of BPO and hydrophobic polymers can be easily prepared. Besides, the presence of high concentration salt in polymer solution makes the electrospinning process complicate due to the distinct increase in ionic conductivity of the solution. However, using BPO as the oxidant can effectively avoid this problem and the

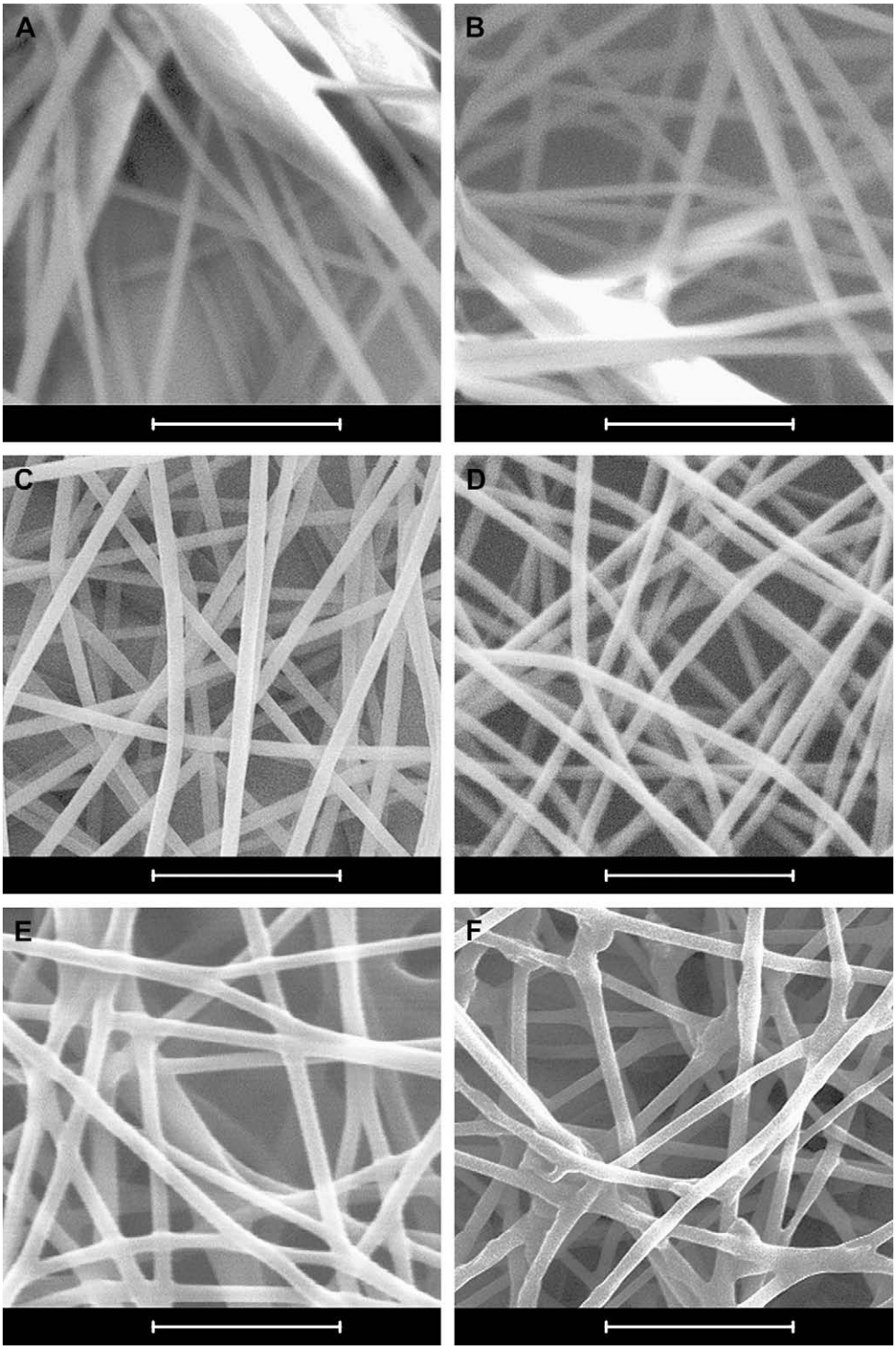

Fig. 1. (A) Typical SEM image of PMMA fibers prepared from the DMF solution of PMMA (60 mg mL^{-1}). (B) Typical SEM image of PMMA fibers prepared from the DMF solution of PMMA (60 mg mL^{-1}) containing a small amount of water (400/1 by volume). (C–F) Typical SEM images of the BPO/PMMA composite fibers prepared from DMF solutions containing 60 mg mL^{-1} PMMA and BPO with concentration of 0.05 M (C), 0.1 M (D), 0.2 M (E) and 0.3 M (F). Scale bar: 5 μm. For the low magnification images, see Fig. S1.

electrospin can be easily controlled. More importantly, the method developed here is a universal approach to CP/HIP composite fiber, and it was tested to be applicable to different hydrophobic polymers (e.g. PMMA and polystyrene (PS)) and CPs (e.g. PPy, poly(3,4-ethylenedioxythiophene) (PEDOT), and polyaniline (PANI)) without significant modification. Furthermore, the preliminary results showed that the PPy/PMMA nanocomposite fibers have potential applications in gas sensing devices.

2. Experimental

2.1. Materials

BPO (25 wt% water), PS ($M_w = 90{,}000\ g\ mol^{-1}$, $d = 1.10$) and PMMA ($M_w = 350{,}000\ g\ mol^{-1}$) were purchased from Alfa Aesar Co., Ltd. Pyrrole was a product of Sinopharm Chemical Reagents Co. Ltd. (Beijing, China) and distilled under reduced pressure before use. 3,4-Ethylenedioxythiophene (EDOT, 99.5%) was bought from Aldrich and used without further purification. Aniline and *N*,*N*-dimethylformamide (DMF) were purchased from Beijing Chemical Reagents Co. (Beijing, China) and used as received.

2.2. Preparation of conducting polymer/hydrophobic insulating polymer (CP/HIP) composite fibers

PMMA solution (60 mg mL^{-1}) was prepared by dissolving 1.2 g PMMA in 20 mL DMF at 50 °C. Then, a controlled amount of BPO was dissolved in the PMMA solution at room temperature to prepare a BPO/PMMA blended solution (the concentration of BPO = 0.05, 0.1, 0.2, or 0.3 M). The blended solutions were electrospun at room temperature under a driving voltage of 9 kV (controlled by a high voltage power source (DW-P303-3AC, Tianjin Dongwen Power Source Plant)). The feeding velocity of the solution was controlled to be 6 mL h^{-1} (SEP 10S, Aitecs). An indium tin oxide (ITO) glass sheet (~10 Ω/Square) or an interdigitated platinum electrode was used as the counter electrode and was placed 10 cm apart from the tip of the capillary. Continuous nanofibers were deposited on the surfaces of counter electrodes and collected in the form of non-woven mats. PS/BPO blended solution (120 mg mL^{-1} with 0.1 M BPO) was prepared following the same procedure, and electrospinning was carried out under a driving voltage of 8 kV.

Typically, to prepare PPy/HIP composite fibers, electrospun HIP fibers (typically 3–10 mg) containing BPO were put into a reaction vessel (500 mL) equipped with an aqueous pyrrole solution (0.2 M, 2.5 mL) and an aqueous hydrochloric acid solution (18 wt%, 2.5 mL) loading reservoirs. The monomer and hydrogen chloride in the reservoirs evaporated gradually and diffused into the BPO/HIP composite fibers where the polymerization was occurred. Composite fibers of PEDOT and PANI were fabricated following the same procedures except that pure EDOT and aniline were used as the vapor sources. After VDP of CPs for a certain period (pyrrole: 30 min, 1 h, 4 h, or 12 h; EDOT: 20 h; aniline: 96 h), the obtained products were collected and dried in air before characterizations.

2.3. Characterization of gas sensing properties

The sensing behavior of the PPy/PMMA composite non-woven mat was characterized by measuring its resistance change upon exposing to NH_3 gas and saturated chloroform vapor at room temperature. The sensor was fabricated by collecting the electrospun fibers onto an interdigitated platinum electrode (10 pairs of digits, 15 μm apart each) and VDP of pyrrole for 4 h. The sensor was connected to a potentiostat (Model 440A, CHI, USA) under computer control to measure the current changes at a constant applied potential (1 V). The probe was kept in a chamber (500 mL) under the applied potential until the current became stable before sensing test. The resistance change towards ammonia was measured by injecting certain volume of saturated ammonia into the chamber. On the other hand, the response to chloroform vapor was determined by inserting the sensor into a chamber filled with saturated chloroform vapor. The response of the sensor was defined as $(R_g - R_0)/R_0$; where R_0 is the resistance of the device before test, and R_g is the resistance after exposing to the analyte.

2.4. Instrumentation

Raman spectra were recorded by the use of an RM 2000 microscopic confocal Raman spectrometer (Renishaw PLC, England) employing a 633-nm laser beam, and a charge coupled device detector with 4 cm^{-1} resolution. IR spectra were recorded on a GX Fourier transform infrared (FTIR) spectrometer (Perkin Elmer, USA) with KBr pellets of the composites. The morphologies of the fibers were imaged with a KYKY 2800 scanning electron microscope (SEM, Beijing, China), operated at 25 kV. Transmission electron microscope (TEM) images were obtained on H-800 electron microscope (Hitachi, Japan). Electric measurements were performed on a 440A potentiostat (CHI, USA).

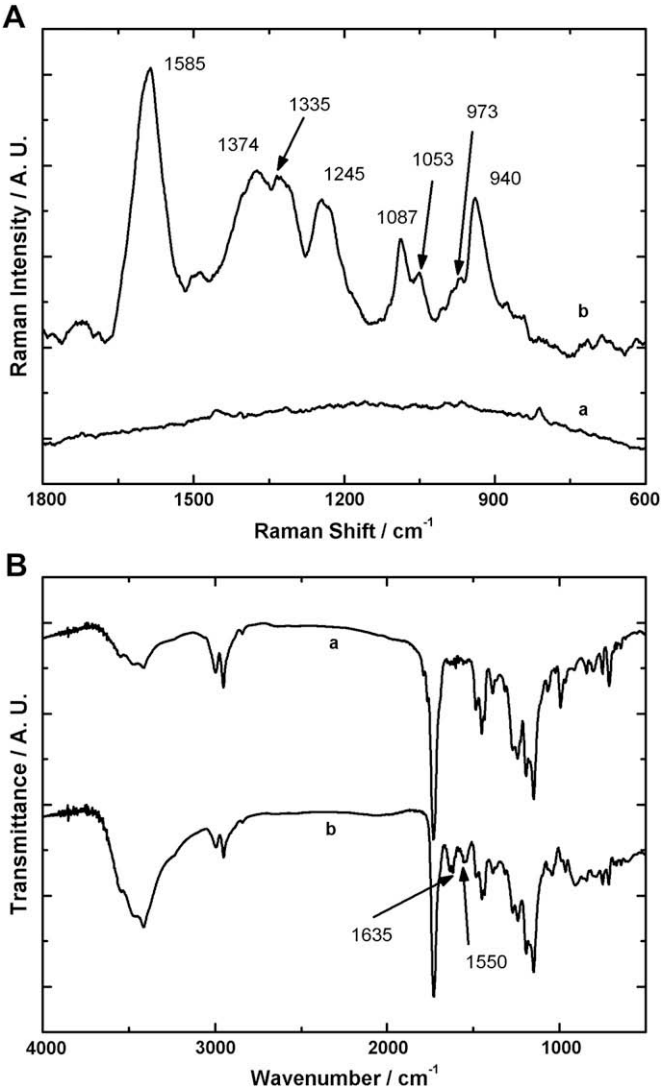

Fig. 2. Raman (A) and IR (B) spectra of BPO10/PMMA (a) and PPy/PMMA composite fibers prepared by VDP of pyrrole on BPO10/PMMA matrix for 4 h (b).

3. Results and discussion

3.1. BPO/PMMA nanofibers

PMMA is a typical hydrophobic polymer and soluble in various organic solvents such as chloroform and DMF, but insoluble in water and methanol. It was reported that PMMA fibers can be prepared by electrospinning its DMF solution [32,33,41]. Furthermore, DMF is a good solvent for wet BPO. Thus, in this work, we chose DMF as the solvent and PMMA concentration was controlled to be 60 mg mL^{-1}, which was reported to have suitable viscosity and surface tension for electrospinning [33]. To find the best condition for obtaining high-quality fibers, solutions containing different contents of BPO were examined. In the case of using pure PMMA solution as the starting material, fibers with beaded structure were produced (Fig. 1A). Usually, the formation of beads can be restrained by adding a small amount of salt into the polymer solution [33]. However, in the present work, upon adding 0.05 or 0.1 M BPO into the PMMA solution, the as-formed fibers (BPO5/PMMA and BPO10/PMMA) also became uniform with average diameters around 450 nm (Fig. 1C and 1D), and no bead was formed during the electrospinning process.

It should be noted here that the commercial available BPO contains 25% water (by weight) for increasing its environmental stability. Thus, it is necessary to make sure whether the small amount of water in the polymer solution was the predominant factor for controlling the morphology of the fibers. As a control experiment, we added water with the same amount as that of 0.05 M wet BPO to PMMA solution for electrospinning. It was found

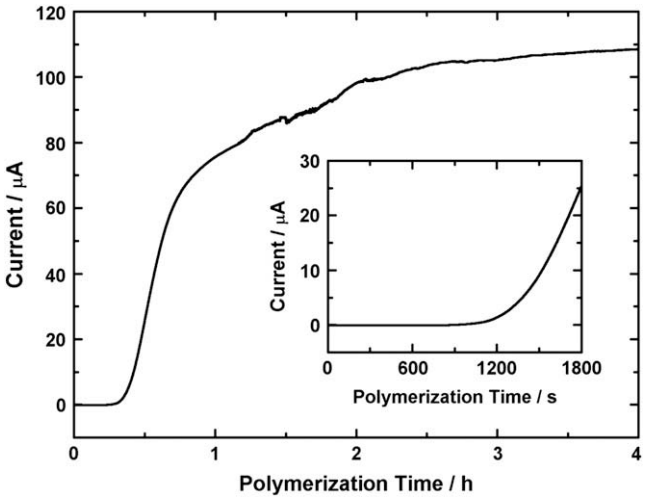

Fig. 4. Time-dependent-current change of a BPO10/PMMA mat exposing in the reaction medium under an applied voltage of 1 V. Inset is the magnification of first 1800 s.

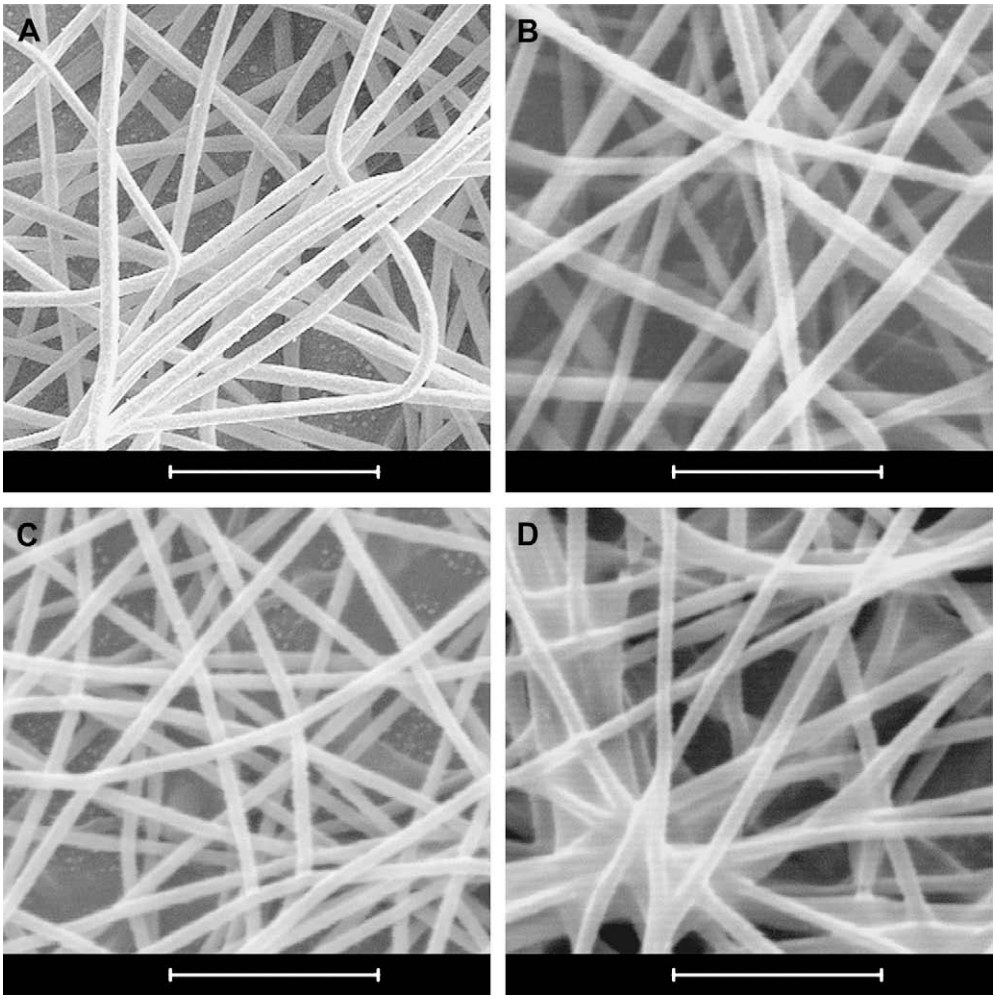

Fig. 3. Typical SEM images of PPy/PMMA composite fibers produced by VDP on BPO10/PMMA for different polymerization time periods. (A) 30 min, (B) 60 min, (C) 4 h, (D) 12 h. Scale bar: 5 μm. For the low magnification images, see Fig. S3.

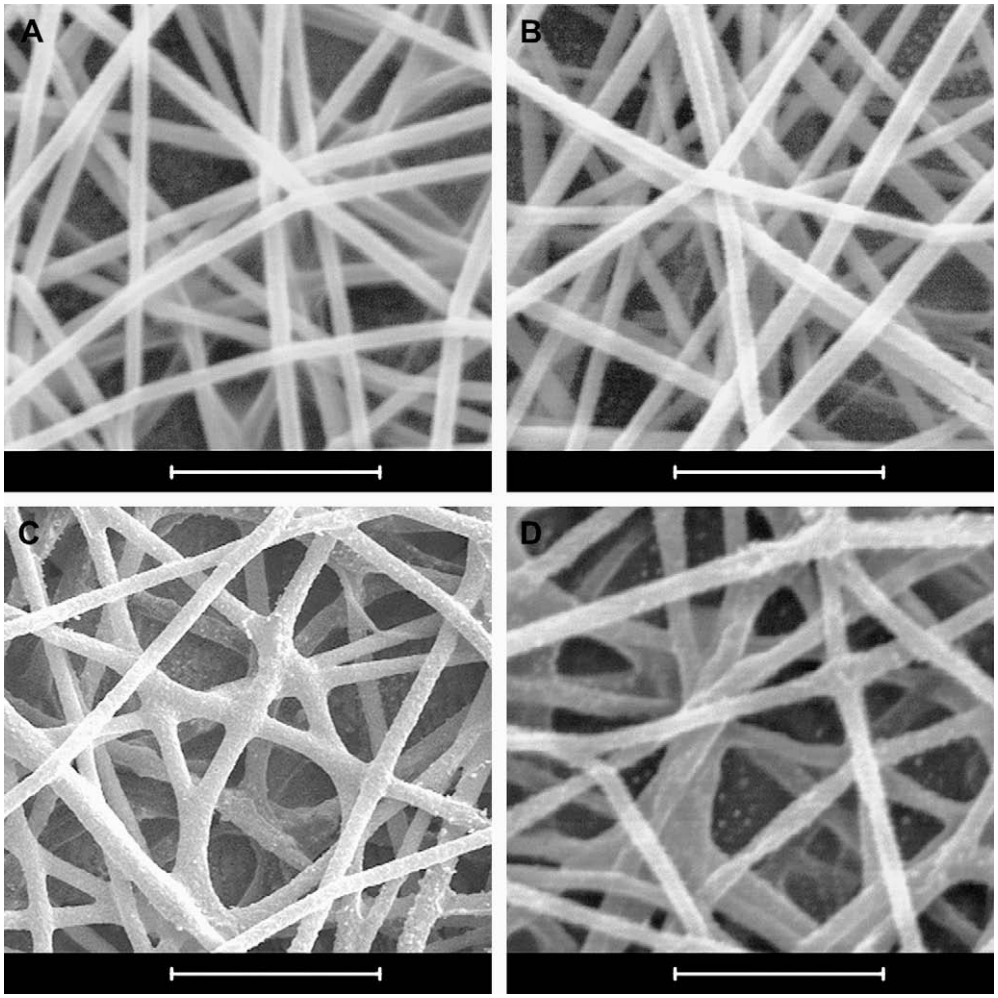

Fig. 5. Typical SEM images of PPy/PMMA composite fibers prepared by VDP on different BPO/PMMA fibers for 4 h. (A) BPO5/PMMA, (B) BPO10/PMMA, (C) BPO20/PMMA, (D) BPO30/PMMA. Scale bar: 5 μm. For low magnification images, see Fig. S4.

that the morphology of the resulting fibers (Fig. 1B) did not show apparent change in comparison with that shown in Fig. 1A. Therefore, it is reasonable to conclude that the morphological change of fibers was induced by the introduction of BPO rather than water. It was reported that the formation of beads is controlled by the viscosity and surface tension of the polymer solution, as well as the net charges carried by the electrospinning jet [42]. To ascertain the principal factor for changing the fiber morphology, the properties of the BPO/PMMA mixed solutions were examined. It was found that the surface tension and viscosity of a PMMA solution

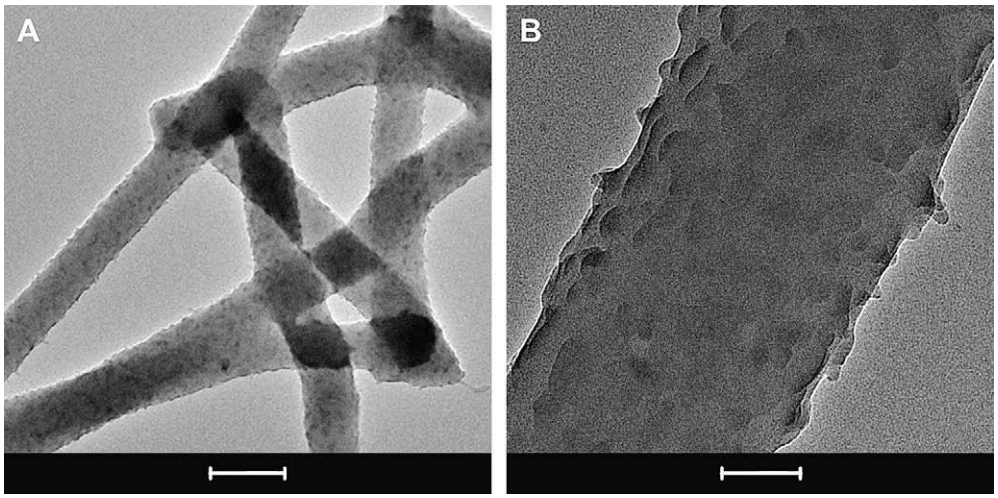

Fig. 6. Typical TEM images of PPy/PMMA fibers prepared by VDP of pyrrole for 4 h on BPO10/PMMA fibers. Scale bar: (A) 500 nm, (B) 100 nm.

were slightly changed by the addition of wet BPO (surface tension: from 36.4 to 36.8 mN m^{-1}, viscosity: from 48 to 49 cP), whereas the conductivity of the solution was increased markedly (from ~3 to 60 μS/cm). Thus, the reduction of bead amount upon addition of BPO would be resulted from the increase of solution conductivity, which consequently increased the net charges carried by the electrospinning jet [25,42]. However, BPO is not an electrolyte and does not have contribution to the solution conductivity. Therefore, the conductivity increase is possibly associated with its reduction product, benzoic acid [40]. If the concentration of BPO was further increased to 0.2 M, the fibers (BPO20/PMMA) were fused together forming nodes at their overlapping spots, indicating that the fibers were still wet when they reached the collecting electrode [43]. Upon further increasing BPO concentration, the amount of nodes was increased and fiber surfaces became rougher (BPO30/PMMA, Fig. 1F). However, the diameters of the fibers altered slightly, and were nearly independent of the BPO concentration.

3.2. PPy/PMMA composite nanofibers

BPO/PMMA composite fibers were used as the templates for VDP of pyrrole. The color of a non-woven mat of BPO/PMMA turned dark soon after being kept in pyrrole and HCl vapors, indicating the formation of PPy. The formation of PPy was further confirmed by spectral examinations. Fig. 2 shows the Raman and IR spectra of the BPO10/PMMA fibers before and after VDP. The Raman spectrum of BPO10/PMMA fibers exhibits only several weak bands in the range of 600–1800 cm^{-1}, whereas after VDP, the spectrum shows typical bands of doped PPy [44,45]. The 1585 cm^{-1} band can be assigned to the C=C stretching mode of PPy backbones, being characteristic of PPy in the oxidized state. The bands around 1374 and 1335 cm^{-1} are associated with the ring stretching of PPy, and the double peaks centered at 1054 cm^{-1} are attributed to C–H in-plane deformation. Bands at 973 and 940 cm^{-1} are assigned to the ring deformation related to bipolarons and polarons, respectively. In IR spectra, most peaks are related to PMMA and BPO components, but the peaks at 1635 and 1550 cm^{-1} only appear in the spectrum of PPy/PMMA, attributing to the C=C stretching of pyrrole rings [46,47].

To optimize the condition for producing high-quality composite fibers, the effects of pyrrole and hydrogen chloride concentrations, polymerization time, and BPO content on the morphology and properties of the final fibers were studied. In typical reactions, a 0.2 M aqueous solution of pyrrole was used as the monomer vapor source. In the system without an HCl vapor source, the polymerization proceeded rather slowly and the mat did not show a visible color change after 4 h VDP. However, due to the slow pyrrole consuming rate, part of pyrrole vapor was condensed on the mat as droplets. The monomer droplets swelled and dissolved the BPO/PMMA matrixes, which made the composite fibers fuse together (Fig. S2A). To accelerate the polymerization rate, an aqueous solution of HCl (18 wt%) was introduced into the reaction system [40]. In this case, the high VDP rate consumed pyrrole vapor effectively. As a result, high-quality PPy/PMMA composite fibers were produced (Fig. 3). On the other hand, as pure pyrrole was used to replace 0.2 M aqueous pyrrole solution as the monomer vapor source (with 18 wt% HCl source), the VDP rate increased greatly (Fig. S2B) and the mat turned black soon after putting it in the reaction vessel. However, exceeding monomer was deposited on the template mat and the BPO10/PMMA fibers were swelled and dissolved during the polymerization process. Finally, a flat composite film was formed within 15 min. Based on the results described above, a 0.2 M pyrrole and a 18 wt% HCl aqueous solutions were tested to be the suitable vapor sources of monomer and acid, correspondingly, for fabricating high-quality PPy/PMMA composite nanofibers.

Fig. 3 shows the SEM images of the PPy/PMMA composite fibers recorded during the process of VDP. In the initial 4 h, the composite fibers kept the outlines of the template fibers (Fig. 3A–C). However, after 12 h polymerization, part of the fibers were fused together as shown in Fig. 3D. These results can be explained as follows: with the elongation of reaction time, VDP rate decreased gradually, due to the decrease of BPO content in the template fibers. In addition, the PPy coating on the fibers also reduced the diffusion rate of the monomer molecules in the fiber matrix. As a result, exceeding unreacted pyrrole monomers were condensed onto the mat as droplets, and polymerized slowly by dioxygen in atmosphere. Fig. 4 plots the current of a BPO10/PMMA nanofiber mat versus VDP time under a constant applied voltage of 1 V. It is clear from this figure that, the current was stable and rather low ($<10^{-10}$ A) in the first 20 min, indicating that continuous PPy conduction-channels did not form in the PMMA matrix. In the period of 20–40 min, a sharp increase in current was observed, signifying the gradual formation of continuous PPy phase. Then, the current underwent a slow increase until reached a stable value after 4 h reaction, indicating a conductive network was well established in the composite fiber mat.

Fig. 5 depicts the morphologies of PPy/PMMA composite fibers formed after 4 h VDP on the fiber templates with different contents of BPO. As BPO5/PMMA and BPO10/PMMA were used as the templates, the resulting fibers maintained the outlines of templates

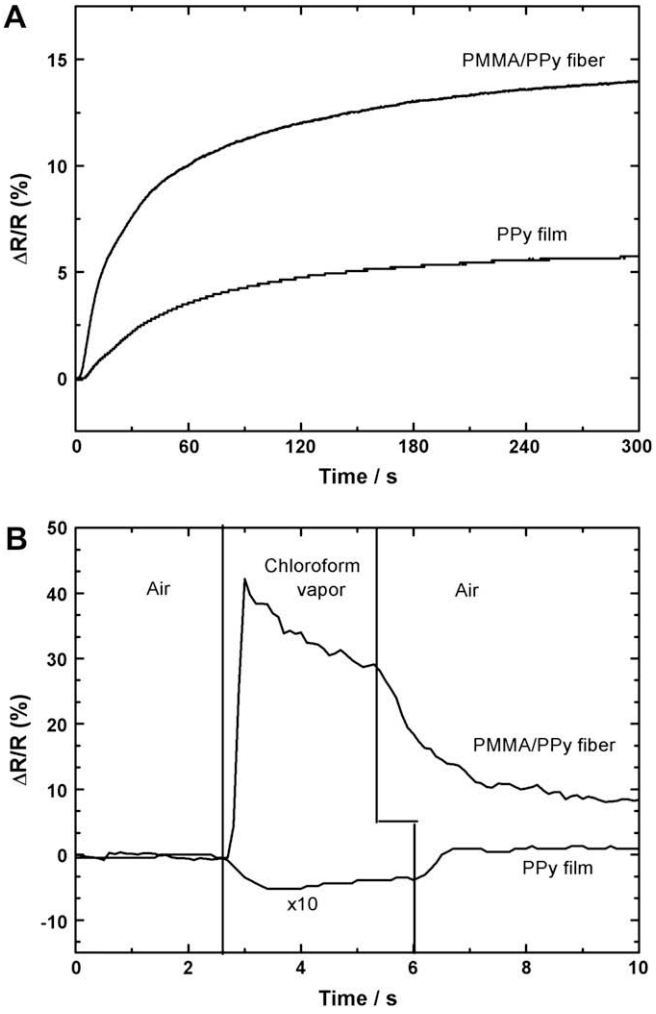

Fig. 7. Resistance change of a PPy/PMMA composite non-woven mat obtained by VDP on BPO10/PMMA for 4 h and a compact PPy film upon exposure in 150 ppm ammonia (A) and saturated chloroform vapor (B).

(Fig. 5A and B) with slight increases in fiber diameters and surface roughness (See Fig. S5). On the other hand, when BPO20/PMMA and BPO30/PMMA templates were used, the resulting PPy/PMMA composite fibers (Fig. 5C and D) showed distinct increases in fiber diameters and surface roughness. Considering the quality of the produced composite fibers and the polymerization rates, PPy/PMMA composite fibers obtained by 4 h VDP with BPO10/PMMA as template were used in further investigations. The PPy content of these PPy/PMMA composite fibers was measured to be 8.2 wt% by elemental analysis (C: 59.54%, H: 7.82, N: 1.77%), and thermo gravimetric analysis results is shown in Fig. S7.

For a composite fiber, it is necessary to confirm whether it is a blend or it has a coaxial-cable-like structure. In a previous work by Jr. Jones and coworkers, coaxial PPy/PMMA cables were fabricated by chemical polymerization of pyrrole on the surfaces of PMMA fibers in an aqueous solution containing both monomer and oxidant [33]. However, in our case, the oxidant, BPO, was distributed in the matrixes of the composite fibers. Moreover, PMMA has good solubility in pyrrole, thus the monomer molecules can diffuse easily into the matrixes of BPO/PMMA fibers. As a result, the PPy/PMMA fibers would not have a well-defined core–shell structure because the polymerization reaction cannot be restricted on the surfaces of the templates. Fig. 6 shows the typical TEM images of PPy/PMMA composite fibers. It is clear from these images that the composite fibers do not have clear core–shell interfaces. Furthermore, we studied the morphology of the composite fibers containing 8.2 wt% PPy after immersing them in chloroform for 12 h to remove their PMMA component (according to a previous report, this process is efficient to remove PMMA core from a core–shell PPy/PMMA composite fiber [33]). The cross-sectional image of the residual fibers also does not show any tube-like structure (See Fig. S6). However, considering the great deformation of the fibers in chloroform, we cannot exclude the possibly existence of a pure PMMA core in the original PPy/PMMA fiber.

3.3. Gas sensing performances of PPy/PMMA nanofiber mats

The high specific surface area and the blend structures of the obtained PPy/PMMA composite fibers endow this material with improved performance in gas sensing. PPy and PMMA components have strong interactions with redox gases and chemical inert organic vapors, respectively. As examples, in the present work, the sensing properties of the composite fibers towards ammonia and chloroform vapor were examined. Fig. 7A shows the time-dependent resistance change of a PPy/PMMA mat (produced from BPO10/PMMA after 4 h VDP) after exposing to 150 ppm ammonia. It can be seen that the resistance of the mat increased by 14% in 300 s. This resistance change was caused by the reduction of oxidized PPy by ammonia [10]. In comparison, under the same condition, the relative resistance change of a compact PPy film was measured to be less than 6%. The enhanced response of the PPy/PMMA non-woven mat is due to its high specific surface area [10].

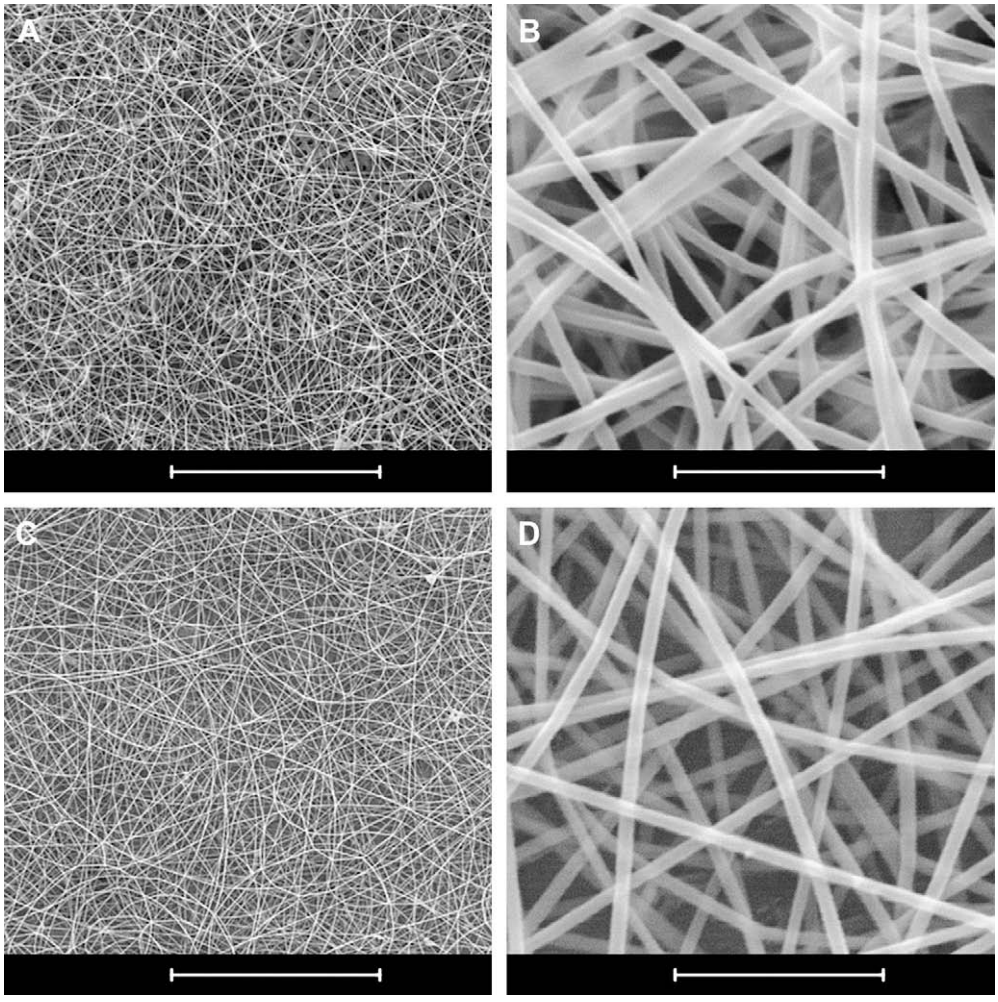

Fig. 8. Typical SEM images of PEDOT/PMMA (A,B) and PANI/PMMA (C,D) composite fibers. Scale bar: (A, C) 50 μm; (B, D) 5 μm.

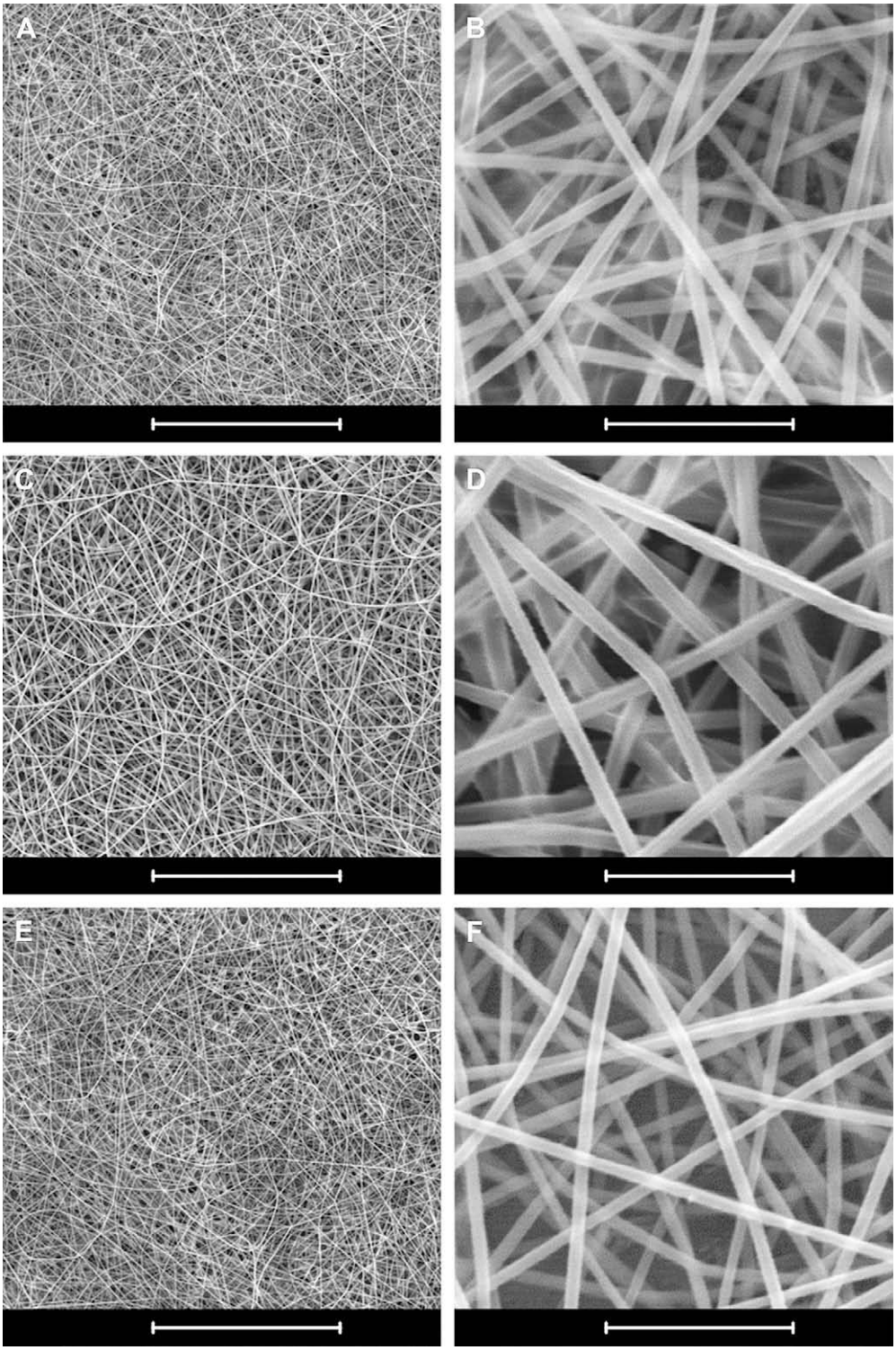

Fig. 9. Typical SEM images of PPy/PS (A, B), PEDOT/PS (C, D) and PANI/PS (E, F) composite fibers. Scale bar: (A, C, E) 50 μm; (B, D, F) 5 μm.

Fig. 7B illustrates the time-dependent resistance change of a PPy/PMMA mat after exposing in a saturated chloroform vapor. It was found that the resistance of the mat increased dramatically, whereas that of the compact PPy film decreased slightly. The response of the composite fibers is over 80 times that of PPy film. The nature of the interactions between CPs and volatile organic compounds (VOCs) and the related influences on the electric resistances of CPs are not very clear now [10]. Chloroform is electrochemically inert to PPy, therefore, the electric resistance change of PPy or its composite should not result from the electron transfer between PPy chains and chloroform molecules. For pure PPy film, a possible explanation for the conductivity increase is that the chloroform molecules diffused into the film and changed the relative permittivity of the film, which will accelerate the electron

hopping between the PPy chains [48]. However, this process became minor in the PPy/PMMA composite due to the presence of PMMA component. PMMA has good solubility in chloroform and when contacting with chloroform vapor, more chloroform molecules can be absorbed in PMMA than pure PPy. Therefore, PMMA component will be swollen by chloroform, leading to the increase of the interchain distances of PPy, and consequently attenuated the electron hopping among polymer chains [49]. Therefore, the synergistic effect of PPy and PMMA is dominant in the sensing mechanism, in which PPy provides electric conductivity while PMMA provides the interaction sites for chloroform. Since the doping levels and the thicknesses of both films were not fully considered, the synergistic effect of PPy/PMMA composite in gas sensing cannot be evaluated accurately. However, these preliminary results indicate that the composite fibers are useful in fabricating gas sensors with high performances.

3.4. Fabrication of other CP/HIP composite fibers

The method described above can be extended to fabricate various CP/HIP composite fibers. We first changed the CP component of the PPy/PMMA composite fibers. PEDOT is an important CP which has wide applications in organic electronic devices, and is usually synthesized by oxidative polymerization of EDOT [50]. EDOT has a higher oxidative polymerization potential and lower vapor pressure in comparison with those of pyrrole, thus the polymerization was carried out using pure EDOT as the monomer vapor source. After 4 h of VDP, the white non-woven mat of BPO/PMMA turned light blue due to the formation of PEDOT. The formation of PEDOT was also confirmed by Raman spectrum (Fig. S8), IR spectrum (Fig. S9) and XPS (Fig. S10). The morphology of the forming PEDOT/PMMA fibers is shown in Fig. 8A and B, in which it can be seen that the PEDOT/PMMA fibers are uniform and the non-woven mat formed by these fibers is defect-free in the scale of 100 μm. PANI/PMMA composite fibers can also be prepared by using aniline as the monomer. However, the polymerization of aniline was found to be slow; mainly due to the formation of crystalline salt from aniline and HCl vapors. A light green film was obtained after reaction for three days, and the formation of PANI was confirmed by its Raman spectrum (Fig. S11). The SEM images of PANI/PMMA are shown in Fig. 8C and D. Both PEDOT/PMMA and PANI/PMMA fibers were conductive (Fig. S12). The successful preparations of PEDOT/PMMA and PANI/PMMA composite fibers prove that the method developed here has wide applications. However, the attempt of preparing PMMA/P3HT was failed, because of the high polymerization potential of 3-hexylthiophene.

On the other hand, other hydrophobic polymer fibers can also be utilized as the templates for the VDP of CPs. Herein, we changed the matrix polymer from PMMA to PS. The electrospinning of PS has been reported in literatures [32,51], in which DMF was proven to be a good solvent for the electrospinning process. Thus, CP/PS composite fibers were obtained by VDP of corresponding monomers on PS/PBO composite fibers electrospun from the DMF solution of 120 mg mL^{-1} PS and 0.1 M BPO. The morphologies of these composite fibers are shown in Fig. 9. It is clear from this figure that all the three types of the composite fibers have uniform morphologies. The formation of PPy, PEDOT and PANI was also confirmed by Raman spectra (Fig. S13–15) and the conductivity increases of the non-woven mats after VDP were also detected (Fig. S16).

4. Conclusions

In conclusion, CP/HIP composite fibers with a blend structure can be fabricated by VDP of aromatic monomer on the electrospun BPO/HIP composite fibers. In this system BPO acted as a liposoluble oxidant. The CP contents in the blend fibers can be controlled by reaction conditions. PPy/PMMA non-woven mat exhibited improved gas sensing performances to ammonia and chloroform vapor compared with those of pure PPy film. This is mainly due to the high specific surface area of the composite fibers and the synergistic effects of hydrophobic PMMA and conductive PPy. The technique developed here is applicable to various CPs and HIPs, and valuable in synthesizing CP nanocomposites with multi-functions.

Acknowledgement

This work was supported by the National Natural Science Foundation of China (50533030, 50873052, 20774056 and 20604013) and 863 Project (2006AA03Z105).

Appendix. Supplementary data

Supplementary data associated with this article can be found in the online version, at doi:10.1016/j.polymer.2009.04.066.

References

[1] Martin CR, Kohli P. Nat Rev Drug Discovery 2003;2(1):29–37.
[2] Abidian MR, Kim DH, Martin DC. Adv Mater 2006;18(4):405–9.
[3] Fu MX, Chen F, Zhang JX, Shi GQ. J Mater Chem 2002;12(8):2331–3.
[4] Yan HL, Zhang L, Shen JY, Chen ZJ, Shi GQ, Zhang BL. Nanotechnology 2006;17(14):3446–50.
[5] Berdichevsky Y, Lo YH. Adv Mater 2006;18(1):122–5.
[6] He XM, Li C, Chen FG, Shi GQ. Adv Funct Mater 2007;17(15):2911–7.
[7] Virji S, Huang JX, Kaner RB, Weiller BH. Nano Lett 2004;4(3):491–6.
[8] Liu HQ, Kameoka J, Czaplewski DA, Craighead HG. Nano Lett 2004;4(4):671–5.
[9] Kemp NT, McGrouther D, Cochrane JW, Newbury R. Adv Mater 2007;19(18):2634–8.
[10] Bai H, Shi GQ. Sensors 2007;7(3):267–307.
[11] Hatchett DW, Josowicz M. Chem Rev 2008;108(2):746–69.
[12] Liu XL, Ly J, Han S, Zhang DH, Requicha A, Thompson ME, et al. Adv Mater 2005;17(22):2727–32.
[13] Wu XF, Shi GQ. J Mater Chem 2005;15(18):1833–7.
[14] Qu LT, Shi GQ. Chem Commun 2004;(24):2800–1.
[15] He YH, Yuan JY, Shi GQ. J Mater Chem 2005;15(8):859–62.
[16] Fu MX, Zhu YF, Tan RQ, Shi GQ. Adv Mater 2001;13(24):1874–7.
[17] Jang J, Chang M, Yoon H. Adv Mater 2005;17(13):1616–20.
[18] Zhang LJ, Wan MX. Adv Funct Mater 2003;13(10):815–20.
[19] Lu GW, Li C, Shi GQ. Polymer 2006;47(6):1778–84.
[20] Reddy KR, Lee K-P, Gopalan AI, Kim MS, Showkat AM, Nho YC. J Polym Sci Part A Polym Chem 2006;44(10):3355–64.
[21] Dong B, Zhong DY, Chi LF, Fuchs H. Adv Mater 2005;17(22):2736–41.
[22] Lu GW, Li C, Shen JY, Chen ZJ, Shi GQ. J Phys Chem C 2007;111(16):5926–31.
[23] Darrell HR, Iksoo C. Nanotechnology 1996;7(3):216–23.
[24] Huang ZM, Zhang YZ, Kotaki M, Ramakrishna S. Compos Sci Technol 2003;63(15):2223–53.
[25] Li D, Xia YN. Adv Mater 2004;16(14):1151–70.
[26] Norris ID, Shaker MM, Ko FK, MacDiarmid AG. Synth Met 2000;114(2):109–14.
[27] Kahol PK, Pinto NJ. Synth Met 2004;140(2–3):269–72.
[28] Kang TS, Lee SW, Joo J, Lee JY. Synth Met 2005;153(1–3):61–4.
[29] Manesh KM, Gopalan AI, Lee K-P, Santhosh P, Song KD, Lee DD. IEEE Trans Nanotechnol 2007;6(5):513–8.
[30] Ji SZ, Li Y, Yang MJ. Sens Actuators B 2008;133(2):644–9.
[31] Jang J, Lim B, Lee J, Hyeon T. Chem Commun 2001;(1):83–4.
[32] Dong H, Nyame V, Macdiarmid AG, Jones WE. J Polym Sci Part B Polym Phys 2004;42(21):3934–42.
[33] Dong H, Jones WE. Langmuir 2006;22(26):11384–7.
[34] De Paoli MA, Waltman RJ, Diaz AF, Bargon J. J Polym Sci, Polym Chem Ed 1985;23(6):1687–98.
[35] Omastova M, Pavlinec J, Pionteck J, Simon F, Kosina S. Polymer 1998;39(25):6559–66.
[36] Nair S, Natarajan S, Kim SH. Macromol Rapid Commun 2005;26(20):1599–603.
[37] Bai H, Li C, Chen F, Shi GQ. Polymer 2007;48(18):5259–67.
[38] Nair S, Hsiao E, Kim SH. J Mater Chem 2008;18(42):5155–61.
[39] Nair S, Hsiao E, Kim SH. Chem Mater 2009;21(1):115–21.
[40] Saravanan C, Shekhar RC, Palaniappan S. Macromol Chem Phys 2006;207(3):342–8.
[41] Piperno S, Lozzi L, Rastelli R, Passacantando M, Santucci S. Appl Surf Sci 2006;252(15):5583–6.
[42] Fong H, Chun I, Reneker DH. Polymer 1999;40(16):4585–92.

[43] Reneker DH, Yarin AL. Polymer 2008;49(10):2387–425.
[44] Furukawa Y, Tazawa S, Fujii Y, Harada I. Synth Met 1988;24:329–41.
[45] Chen F, Shi GQ, Fu MX, Qu LT, Hong XY. Synth Met 2003;132(2):125–32.
[46] Bazzaoui M, Bazzaoui EA, Martins L, Martins JI. Synth Met 2002;130(1):73–83.
[47] Fredj HB, Helali S, Esseghaier C, Vonna L, Vidal L, Abdelghani A. Talanta 2008;75(3):740–7.
[48] Vercelli B, Zecchin S, Comisso N, Zotti G, Berlin A, Dalcanale E, et al. Chem Mater 2002;14(11):4768–74.
[49] Ruangchuay L, Sirivat A, Schwank J. Talanta 2003;60(1):25–30.
[50] Groenendaal L, Jonas F, Freitag D, Pielartzik H, Reynolds JR. Adv Mater 2000;12(7):481–94.
[51] Stephens JS, Frisk S, Megelski S, Rabolt JF, Chase DB. Appl Spectrosc 2001;55(10):1287–90.